

Stimulating the Substrate Folding Activity of a Single Ring GroEL Variant by Modulating the Cochaperonin GroES^{*S}

Received for publication, April 28, 2011, and in revised form, July 8, 2011. Published, JBC Papers in Press, July 10, 2011, DOI 10.1074/jbc.M111.255935

Melissa Illingworth, Andrew Ramsey, Zhida Zheng, and Lingling Chen¹

From the Department of Molecular and Cellular Biochemistry, Indiana University, Bloomington, Indiana 47405

In mediating protein folding, chaperonin GroEL and cochaperonin GroES form an enclosed chamber for substrate proteins in an ATP-dependent manner. The essential role of the double ring assembly of GroEL is demonstrated by the functional deficiency of the single ring GroEL^{SR}. The GroEL^{SR}-GroES is highly stable with minimal ATPase activity. To restore the ATP cycle and the turnover of the folding chamber, we sought to weaken the GroEL^{SR}-GroES interaction systematically by concatenating seven copies of *groES* to generate *groES*⁷. GroES Ile-25, Val-26, and Leu-27, residues on the GroEL-GroES interface, were substituted with Asp on different *groES* modules of *groES*⁷. GroES⁷ variants activate ATP activity of GroEL^{SR}, but only some restore the substrate folding function of GroEL^{SR}, indicating a direct role of GroES in facilitating substrate folding through its dynamics with GroEL. Active GroEL^{SR}-GroES⁷ systems may resemble mammalian mitochondrial chaperonin systems.

The Hsp60 chaperonin family is ubiquitous among the three kingdoms of life. The paradigm *Escherichia coli* GroEL is the well characterized Hsp60 chaperonin that, together with cochaperonin GroES, uses ATP to assist a variety of proteins to fold in the cell (1–6). Both GroEL and GroES are essential for cell viability (7). Fourteen identical GroEL subunits assemble into a cylindrical structure of two heptameric rings stacked back to back, with a functional central cavity at either end (8). Each GroEL subunit is organized into three domains. The apical domains, located on the opening of the rings, form the main substrate-binding site and interact with GroES. The equatorial domains, situated in the center of the cylindrical GroEL, provide most of the intra-ring and all the inter-ring subunit interactions and contain the nucleotide-binding site. The intermediate domains connect the apical and the equatorial domains, transmitting signals including substrate binding and nucleotide effect across the subunits. The surface lining the GroEL central cavity is mainly hydrophobic, and this hydrophobic character has been shown to be important for capturing and interacting with misfolding protein substrates (9–12). The homoheptameric GroES adopts a dome-like assembly with each monomer folding into a β -barrel structure flanked by a structurally flexible loop termed the GroES mobile loop (13, 14). In the presence

of nucleotides, GroES forms a stable asymmetric bullet-shaped GroEL-GroES complex (see Fig. 1A inset) (15–18). The crystal structure of GroEL-ADP₇-GroES shows that binding of GroES converts the GroEL central cavity to an enclosed chamber (termed the *cis* complex) (19). Three hydrophobic GroES residues (Ile-25, Val-26, and Leu-27), of the GroES mobile loop, interact with residues from the GroEL apical domain (see Fig. 1A), and the GroES-GroEL interface is largely hydrophobic. Binding of GroES to one GroEL ring transforms the surface of the GroEL central cavity from hydrophobic, favorable for binding misfolded substrate proteins, to folding promoting hydrophilic.

The double ring assembly of GroEL is essential for the GroE-assisted protein folding reaction. The substrate protein initiates folding within the isolated folding favorable environment upon displacement from the wall of the GroEL central cavity due to GroES association and is released outside the GroE capsule following GroES departure. Both dissociation and association of GroES are ATP-driven and are mediated by the intricate and highly coordinated cross-ring allostery. ATP hydrolysis in the GroES-bound GroEL ring (*cis* ring) weakens GroES-GroEL interaction (20); however, the hydrolysis product, GroES-GroEL^{cis}-ADP₇-GroEL^{trans}, is still very stable with a dissociation constant (K_d) of 0.1–26 nM (16, 21–23). To finally discharge GroES from the *cis* ring, thereby releasing the folding substrate, binding of ATP to the other (*trans*) GroEL ring is required (20, 24, 25). The newly ATP-charged *trans* ring, which is prone to GroES association, becomes a “new” folding active *cis* chamber, whereas the collapsing *cis* chamber assumes inactive state. Thus, in assisting protein folding, the two GroEL rings communicate to alternate between folding active and inactive states, and GroEL functions as a two-stroke molecular machine (1, 26–28).

Consistent with the essential role of the two ring architecture of GroEL in cycling the folding active *cis* chamber, a single ring (SR)² version GroEL (29), termed GroEL^{SR} in our study here, is functionally impaired. Although GroEL^{SR} and GroES may form the folding chamber for substrate proteins to undergo and complete folding, substrate proteins are not released from the chaperonin system (20, 30–32). Dissociation of the GroEL^{SR}-GroES complex is very slow (the half-life $t_{1/2}$ of GroEL^{SR}-GroES is ~300 min) (29), due to the lack of the allosteric effect originating from ATP binding to the absent *trans* ring (above). As a result, the highly stable GroEL^{SR}-GroES complex traps the folding substrate proteins, stalling

* This work was supported, in whole or in part, by National Institutes of Health Grants R01GM065260 and R01GM065260-05S1 (to L. C.).

^S The on-line version of this article (available at <http://www.jbc.org>) contains supplemental Figs. S1 and S2.

¹ To whom correspondence should be addressed: Dept. of Molecular and Cellular Biochemistry, 212 S. Hawthorne Dr., Simon Hall 400A, Indiana University, Bloomington, IN 47405. E-mail: linchen@indiana.edu.

² The abbreviations used are: SR, single ring; MDH, malate dehydrogenase; mt, mitochondrial.

Activating GroEL^{SR} via GroEL-GroES Interaction

the chaperonin reaction cycle. Thus, GroEL^{SR} is unable to substitute GroEL for cell growth (33).

Recently, active single ring chaperonin systems have been reported. The folding active GroEL^{SR}-GroES systems consist of variants of GroEL^{SR}, identified from genetic analysis (34–37), or variants of GroES, identified from random mutagenesis study on the GroEL-binding GroES mobile loop (36). Reduced GroEL-GroES interaction has been implicated in these folding active GroEL^{SR}-GroES variants; however, the basis for the mutational effect is not immediately clear. For example, the affected GroEL residues are not located on the GroEL-GroES interface and most likely interfere with the ATP-driven, highly coordinated structural transitions that are obligated in the GroE reaction. Intriguingly, the weakened GroEL-GroES interaction in these folding active single ring chaperonin systems is reminiscent of mammalian mitochondrial chaperonin mtHsp60-mtHsp10 system. mtHsp60 exists as a single heptameric ring in solution (38), and may function as single ring (23, 39), although a mechanism involving a transiently associated double ring has been proposed (40, 41). Moreover, the mtHsp60-mtHsp10 interaction appears to be transient in the presence of ADP (23).

In this study, we directly explored the notion that weakened GroEL-GroES interaction may restore the substrate folding function of GroEL^{SR}. We took a unique strategy to create GroES variants with various affinities for GroEL in a systematic and controlled manner. We constructed a covalently linked GroES variant, *groES*⁷, so that we could independently substitute residues in individual GroES subunits. We examined these GroES⁷ variants for their function with both the double ring GroEL and the single ring GroEL^{SR}. In addition to the mechanistic understanding of how a GroEL ring assists protein folding, studies of active GroEL^{SR}-GroES systems may provide useful information on the mechanism of mtHsp60-mtHsp10 in mammalian mitochondria.

EXPERIMENTAL PROCEDURES

Construction of *groES*⁷ and Its Mutants—To construct the covalently connected *groES*⁷, *groES* was amplified with primers including the desired restriction site sequences, to generate seven *groES* containing DNA fragments: *groES1* (with NdeI and KpnI), *groES2* (with KpnI and XhoI), *groES3* (with XhoI and Sall), *groES4* (with Sall and SacI), *groES5* (with SacI and BamHI), *groES6* (with BamHI and EagI), and *groES7* (with EagI and HindIII). *groES1* and *groES2* were digested with KpnI, purified, and ligated to generate the *groES1-groES2* fragment, which was further amplified by PCR for a sufficient quantity. Fragments of *groES3-groES4* and *groES5-groES6-groES7* were generated in a similar manner, and so was the *groES1-...-groES7* fragment, which was digested with NdeI and HindIII and inserted into a modified pET28b vector, whose region between HindIII and Bpu was replaced with a short DNA oligonucleotide. To generate GroES⁷ mutants, a mutation was first introduced into the regular *groES* construct using QuikChange kit (Stratagene). The mutated *groES* was amplified with primers including the desired restriction site sequences and ligated to a TOPO vector (Invitrogen). The circularized TOPO vector was transformed into TOP10 cells for amplification and digested

with specific restriction enzymes to generate the *groES* mutant gene with defined restriction cuts, which was inserted via the corresponding sites into the *groES*⁷ pET28b construct. DNA sequencing was performed on the entire *groES*⁷ gene to confirm that mutation was only on the designated module(s). When expressed, GroES⁷ has a His₆ tag on the N terminus of the protein.

Protein Expression and Purification—*groES*⁷ pET28b was transformed into BL21DE3 for overexpression. Cells were grown in LB medium until A₆₀₀ reached 0.6, induced with 0.4 mM isopropyl 1-thio-β-D-galactopyranoside, and continued for 4–5 h. Cells were re-suspended in 10 mM sodium phosphate, pH 7.5, 500 mM NaCl, and 10 mM imidazole, and lysed using a microfluidizer (Microfluidics). The clear cell lysate was loaded onto a Ni affinity column, and GroES⁷ was eluted with a linear gradient of imidazole (5–500 mM). The GroES⁷-containing fractions were combined, concentrated, dialyzed to 50 mM Tris-Cl, pH 7.5, and loaded onto a FastQ column (GE Healthcare), and GroES⁷ was eluted with a linear gradient of NaCl (0–1 M). The GroES⁷-containing fractions were combined, concentrated, dialyzed to 50 mM Tris-Cl, pH 7.5, and loaded onto a Superdex 200 gel filtration column (GE Healthcare).

Cell growth and protein purification of GroEL and GroEL^{SR} were similar, as described in Ref. 42. A purification step using 30% methanol followed by an additional size exclusion chromatography was included to ensure high quality of GroEL and GroEL^{SR}, and tryptophan fluorescence confirmed the absence of bound peptides. Protein expression and purification of wild-type and GroES mutants were based on the previous procedures (19).

ATPase Assay—The steady-state ATP hydrolysis rate was measured using the malachite green assay (43). GroEL or GroEL^{SR} was added to TEA buffer (50 mM triethanolamine, pH 7.5, 50 mM KCl, and 20 mM MgCl₂) to a final concentration of 0.125 μM (tetradecameric GroEL) or 0.25 μM (heptameric GroEL^{SR}). The final concentration of GroES (heptamer) and GroES⁷ proteins was 0.3 μM. The solution was incubated at 25 °C for 10 min. The hydrolysis was initiated by addition of 100 mM pH 7.0 ATP to a final concentration of 2 mM and followed every 2 min for 12 min using the malachite green assay.

Malate Dehydrogenase (MDH) Refolding Assay—MDH was unfolded in TEA buffer including 3 M GdmHCl to a final concentration of 36.7 μM (monomeric MDH). To refold MDH, 2.75 μl of unfolded MDH was diluted at 1:100 (v/v) to a final volume of 275 μl of refolding solution (at 30 °C) containing 50 mM TEA, pH 7.4, 50 mM KCl, 1 mM ATP, and 1 μM tetradecameric GroEL (or 2 μM heptameric GroEL^{SR}) with 4 μM or without GroES. At desired time intervals, 20 μl of reaction solution was removed and mixed with 1 ml of NADH assay solution (50 mM Tris-Cl, pH 7.4, 10 mM DTT, 0.2 mM NADH, 1 mM ketomalonate), and absorption at 340 nm was taken to monitor the decrease of NADH (44). As a positive control, activity of 367 nM native MDH (monomeric concentration) was measured at the same time intervals and was taken as 100% activity. Refolded and active MDH converts NADH to NAD⁺.

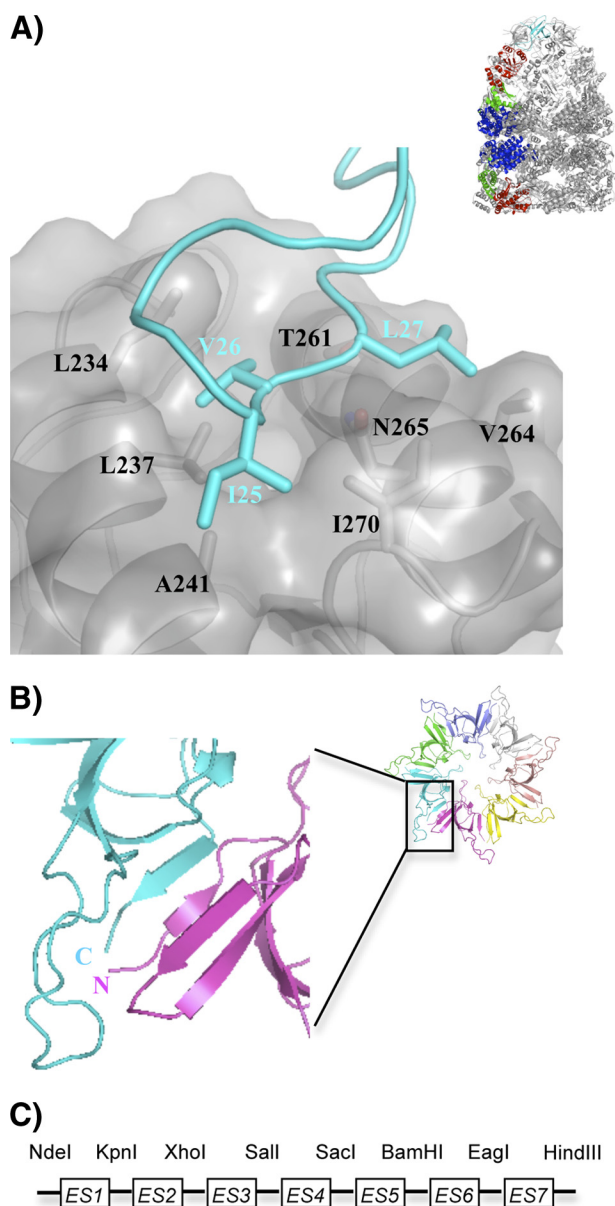


FIGURE 1. *A*, GroES-GroEL interface. The three GroES residues (Ile-25, Val-26, and Leu-27) interact directly with GroEL residues. Side chains of the interacting residues are shown. *Inset*, the crystal structure of GroEL-GroES (Protein Data Bank ID code 1AON). One GroEL subunit in both *cis* and *trans* rings is highlighted with *red* for the apical domain, *green* for the intermediate domain, and *blue* for the equatorial domain. One subunit of GroES is colored in *cyan*. *B*, close proximity of N and C termini of neighboring GroES subunits in the homoheptameric GroES. *Inset*, top view of GroES (Protein Data Bank ID code 1AON). *C*, construct of *groES*⁷ with the distinctive enzymatic sites flanking ends of the individual *groES* genes, denoted as ES1, ES2...ES7.

RESULTS

Essential Role of GroES Ile-25 and Leu-27—To decrease GroEL-GroES interaction, the three GroEL-interacting residues, Ile-25, Val-26, and Leu-27, on the GroEL-GroES interface (Fig. 1A) were individually substituted to Asp, resulting in GroESI25D, GroESV26D, and GroESL27D variants. When incubated with GroEL in the presence of ADP, both GroESI25D and GroESL27D variants could not form a stable complex with GroEL; they were largely absent by SDS-PAGE analysis on the GroEL-containing fractions (supplemental Fig. S1A). Interestingly, the GroESV26D variant, albeit containing a total of seven

substitutions in heptameric form, could still form the GroEL-GroES complex, as suggested by SDS-PAGE (supplemental Fig. S1A). Previous studies show that in forming a complex with GroEL, GroES inhibits the ATP hydrolysis rate of GroEL by ~50% (16, 21, 45, 46). Neither GroESI25D nor GroESL27D variants altered GroEL ATP hydrolysis significantly (supplemental Fig. S1B), whereas the GroESV26D variant reduced GroEL ATPase function in a manner similar to the wild-type GroES. These findings are consistent with the model that both GroESI25D and GroESL27D variants did not associate with GroEL, whereas GroESV26D formed a stable complex with GroEL. To further confirm the mutational effects, the GroES variants were subjected to a substrate protein folding study. The spontaneous folding of MDH is low (~5%), and the complete chaperonin system, including GroEL, GroES, and ATP, is required to achieve efficient MDH folding (47), indicating that formation of the folding active GroEL-GroES chamber is essential for MDH folding. Supplemental Fig. S1C shows that neither GroESI25D nor GroESL27D supported GroE-assisted MDH folding, suggesting that both variants were not able to form a functional complex with GroEL. As expected, folding of MDH using GroESV26D was as efficient and effective as using the wild-type GroES, indicating formation of the GroESV26D-GroEL complex. Taken together, these findings confirm the critical function of GroES residues Ile-25 and Leu-27 in GroEL-GroES interaction and indicate a minor role of GroES Val-26 in complex formation.

We next examined whether the observed mutational effects of I25D, V26D, and L27D on GroEL-GroES interaction were applicable to the GroEL^{SR}-GroES system. GroES inhibits the ATP hydrolysis rate of GroEL^{SR} by up to ~90% (29). As shown in supplemental Fig. S1B, GroESV26D decreased the ATPase activity of GroEL^{SR} to a level comparable with that of wild-type GroES. In contrast, both GroESI25D and GroESL27D did not affect the ATP hydrolysis rate of GroEL^{SR}. These results are parallel to those using GroEL, further substantiating the importance of Ile-25 and Leu-27, in contrast to the minimal role of Val-26, in GroEL-GroES interaction. These observations are consistent with results of sequence analysis on 31 GroES homologous proteins from prokaryotes to eukaryotes (48). Ile and Leu are highly conserved at position 25 (96% of sequences) and position 27 (94%), respectively, whereas the amino acid at position 26 is more diverse: Val (48%), Ile (29%), Leu (10%), Met (7%), Phe (3%), and Gln (3%).

When assaying for MDH folding activity, we found that none of the three mutants was able to cooperate with GroEL^{SR} to assist MDH folding; however, the inactivation mechanisms are different. Considering the similar binding affinities of GroESV26D and GroES for GroEL, the observed limited MDH folding using GroESV26D should be most likely due to the folding MDH trapped within the nondissociable GroESV26D-GroEL^{SR} complex. On the other hand, given the abolishing effect of I25D or L27D mutation on GroEL-GroES interaction, the minimal MDH activity observed with GroESI25D or GroESL27D and GroEL^{SR} is most likely due to the lack of formation of the folding chamber, which is essential for MDH folding (47). Thus, straightforward manipulations on the GroEL-interacting residues of Ile-25, Val-26, and Leu-27 cannot confer the single ring

Activating GroEL^{SR} via GroEL-GroES Interaction

GroEL^{SR} the sustainable substrate folding activity because the required enclosed folding chamber either is nonrecyclable (in the case of GroESV26D) or does not form (in the case of GroESI25D and GroESL27D). Alternatively, for GroESV26D, it might also be likely that its presumably decreased affinity for GroEL, although subtle, could not completely displace the protein substrate into the central cavity for folding (see "Discussion").

Modulating GroES Affinity for GroEL—The abolished GroEL-GroES interaction observed in GroESI25D and GroESL27D may be explained by the 7-fold amplified mutational effect because a single gene modification in *groES* transforms into seven amino acid substitutions in the GroES heptamer. We reasoned that if some of the seven GroES subunits maintained the wild-type sequence, the resulting GroES variants would display different levels of reduced affinities for GroEL. We hypothesized that these GroEL-binding compromised GroES variants might cooperate with GroEL^{SR} to complete the chaperonin reaction cycle.

To modify an individual GroES subunit, we took advantage of the observation that the N and C termini of neighboring GroES subunits in heptameric GroES are within 5 Å (*C α -C α* distance) (19) (Fig. 1B) and created a synthetic gene, *groES*⁷, concatenating seven copies of the *groES* gene (Fig. 1C). The expressed protein, GroES⁷, consists of seven GroES modules, corresponding to the seven GroES subunits in the canonical GroES homoheptamer, in one contiguous polypeptide chain. Linker sequences of four amino acids (consisting of Gly, Ser, or Ala) give flexibility between subunits. Distinct restriction sites are designed to flank each *groES* gene, so that modifications can be introduced into the specific position(s) of the desired module(s). We used *groES*⁷ to incorporate I25D or L27D substitutions in specific GroES modules, to create GroES⁷ variants with a range of weakened affinities for GroEL.

GroES⁷ Behaves Like GroES—To examine the effect of the peptide linkers tethering neighboring GroES modules, we compared the structural and functional aspects of GroES⁷ with the canonical GroES heptamer. GroES⁷ (theoretical molecular mass of 76,721 Da) migrated as a molecular species with the molecular size of 82.2 kDa estimated from gel filtration chromatography, whereas the molecular size of the canonical GroES heptamer (theoretical molecular mass of 72,723 Da) was estimated to be 71.3 kDa by gel filtration. Like GroES, GroES⁷ formed a complex with GroEL in the presence of nucleotides, as assayed by SDS-PAGE analysis (Fig. 2A). GroES⁷ decreased ATPase activity of GroEL to a level comparable with that using GroES (Fig. 2B). Moreover, GroES⁷ assisted MDH refolding in a manner similar to GroES, with comparable reaction kinetics and refolding yield (Fig. 2C). The resemblances of GroES⁷ to GroES were extended to their interaction with GroEL^{SR}. As shown in Fig. 2B, GroES⁷ diminished ATPase activity of GroEL^{SR} to a level similar to that using GroES (~10% of the intrinsic rate of GroEL^{SR}). Like GroES, GroES⁷ could only support the minimal MDH folding by GroEL^{SR} (Fig. 2C). Taken together, these data show that the covalently linked single chain GroES⁷ is similar to the wild-type GroES in all the measures examined. Studies using the covalently linked GroES have been

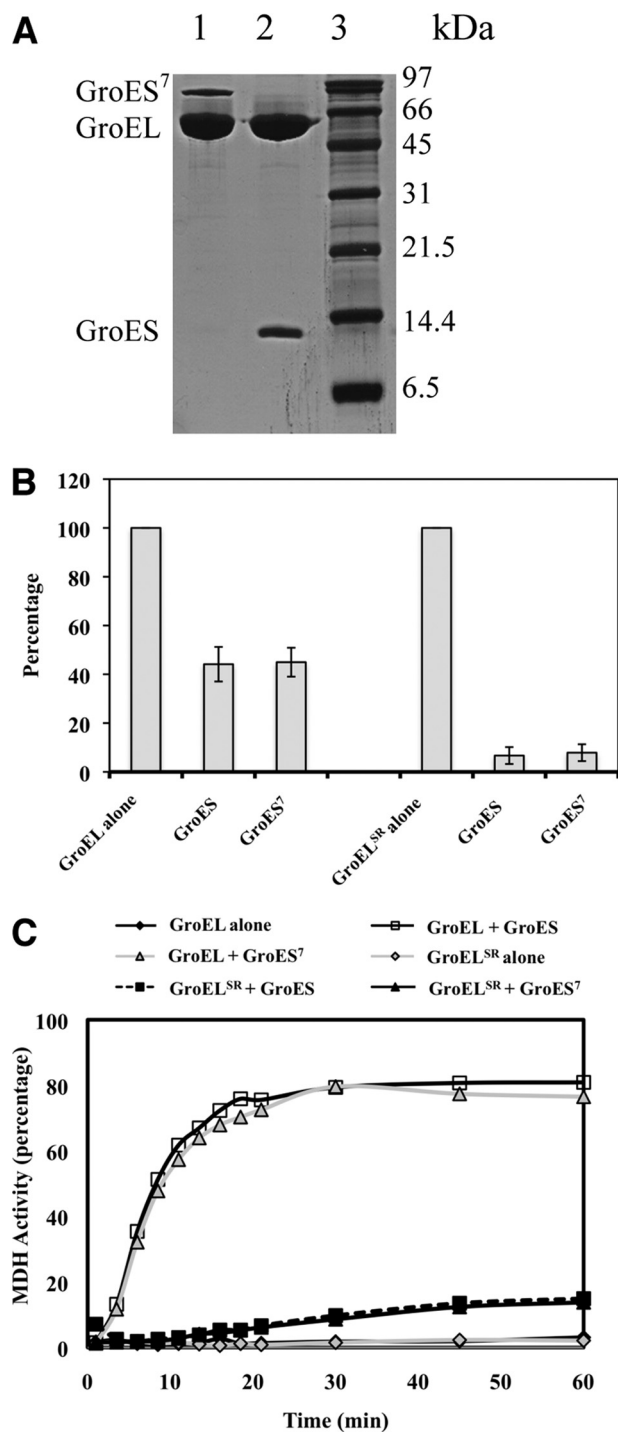


FIGURE 2. GroES⁷ behaves like the wild-type GroES. A, GroES⁷ forms a complex with GroEL by SDS-PAGE analysis. Lane 1, GroEL-GroES⁷ complex; lane 2, GroEL-GroES complex; lane 3, molecular mass markers. Complex formation, separation, and analysis are the same as those in [supplemental Fig. S1A](#). B, effect of GroES⁷ on the steady-state ATPase activities of GroEL and GroEL^{SR}. The intrinsic ATP hydrolysis rate of GroEL was set as 100% for the GroEL group, and that of GroEL^{SR} was set as 100% for the GroEL^{SR} group. S.D. values (error bars) are calculated from multiple (at least three) experiments using proteins from different purifications. C, GroES⁷ in GroEL- and GroEL^{SR}-mediated MDH refolding. At least three independent experiments were carried out using proteins from different batches of purification. Shown here are representative MDH refolding reactions.

reported, and the additional peptide linkers are found not to have functional interference (49, 50).

GroES⁷ Variants Impair Substrate Folding of GroEL—Given that seven I25D and L27D substitutions on GroES completely disrupted GroEL-GroES interaction, we introduced the substitutions at subsets of GroES modules in GroES⁷, with the intention to generate GroES⁷ variants with a range of weakened affinities for GroEL. So far, we have created mono-, di-, and tri-substituted GroES⁷ variants as follows: GroES⁷I25D₁, GroES⁷I25D_{1,4}, and GroES⁷I25D_{1,4,7}; GroES⁷L27D₁, GroES⁷L27D_{1,4}, and GroES⁷L27D_{1,4,7}. (The subscripts denote the modified GroES module(s) in GroES⁷.) As a comparison, we also prepared V26D substitutions: GroES⁷V26D₁, GroES⁷V26D_{1,4}, and GroES⁷V26D_{1,4,7}; the GroES⁷V26D variants were not expected to have altered affinity for GroEL.

Compared with the completely depleted inhibition of GroES I25D or GroES L27D on GroEL ATPase activity, substitutions of I25D and L27D in GroES⁷ generated a range of effects on GroEL ATP hydrolysis rates. In both the GroES⁷I25D and GroES⁷L27D series, GroEL ATPase activity increased with the number of substitution (Fig. 3A). When three substitutions were incorporated into GroES⁷ as in GroES⁷I25D_{1,4,7} and GroES⁷L27D_{1,4,7}, the inhibition changed from 50% to 10–20% of the intrinsic GroEL ATP hydrolysis rate. Because a large inhibition may presumably be correlated with the strong GroEL-GroES interaction, these findings suggest that the substituted GroES⁷ variants display different affinities for GroEL and that they do not interact with GroEL as strongly as the wild-type GroES. As expected, V26D substitutions in GroES⁷ did not alter GroES function, as variants of GroES⁷V26D affected GroEL ATPase activity in a manner similar to GroES (supplemental Fig. S2A).

Given that variants of GroES⁷I25D and GroES⁷L27D inhibited GroEL ATPase activity to various extents, we next investigated how the altered ATP hydrolysis rate of the modified chaperonin system influenced MDH folding. A single substitution of GroES⁷I25D₁ slowed the MDH folding rate but with a slightly decreased folding yield over a time course of 60 min (Fig. 3B). A further substitution, GroES⁷I25D_{1,4}, decelerated the rate of MDH folding drastically and reduced the final yield by ~28% (60% compared with 77% using the wild-type system). Folding of MDH became modest when using GroES⁷I25D_{1,4,7}, the tri-substituted GroES⁷ variant. The observations that both the folding rate and the final yield of MDH declined with the increasing number of the affected GroES modules were also found in the GroES⁷L27D series (Fig. 3C). Note that MDH folding appears to be more sensitive to I25D substitution in GroES⁷ than to L27D substitution; with the same number of affected modules, variants of I25D substitution resulted in greater reduction of both MDH folding rate and folding yield than those of L27D substitution. These findings suggest that residue Ile-25 plays a more important role than Leu-27 in MDH folding, although their differential effect on GroEL ATP hydrolysis rate was not evident (Fig. 3A). As expected, the mono-, di-, and tri-V26D substitutions in GroES⁷ did not affect MDH folding (supplemental Fig. S2C).

Increase of ATPase Rate in GroEL^{SR}-GroES⁷ Systems—Given that variants of GroES⁷I25D and GroES⁷L27D decreased inhi-

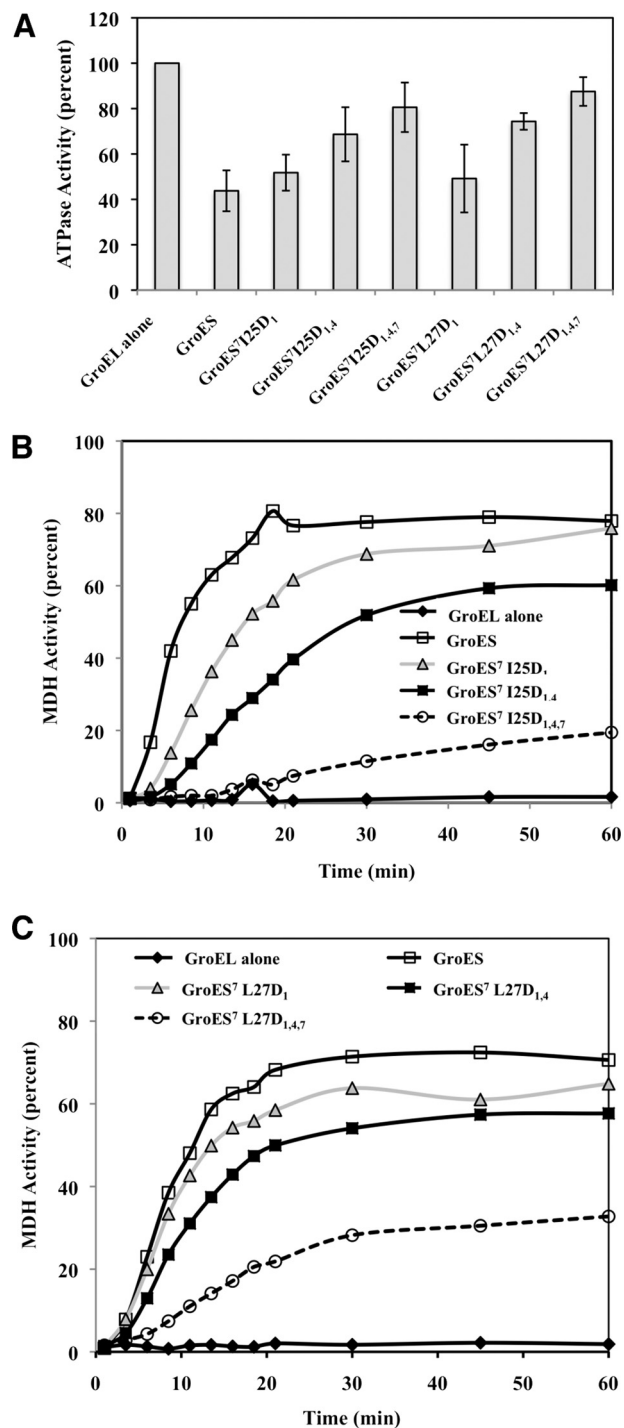


FIGURE 3. Effects of GroES⁷I25D and GroES⁷L27D variants on GroEL. A, steady-state ATPase activity. B and C, MDH folding activity. For the ATPase experiments, the intrinsic GroEL ATP hydrolysis rate was set as 100%. Experiments were repeated at least three times, and S.D. values are shown (error bars). For the MDH folding assay, activity of native MDH was set as 100%. Experiments were repeated multiple times, and data of representative runs are shown here.

bition on ATP hydrolysis of GroEL, we next investigated whether these variants restored the diminishing ATPase activity of GroEL^{SR}-GroES. A single I25D substitution in GroES⁷ alleviated the GroES-stalled ATP hydrolysis of GroEL^{SR} (~7%) to ~18% of the intrinsic rate of GroEL^{SR} (Fig. 4A). The GroES⁷I25D_{1,4} variant with two substitutions further relieved

Activating GroEL^{SR} via GroEL-GroES Interaction

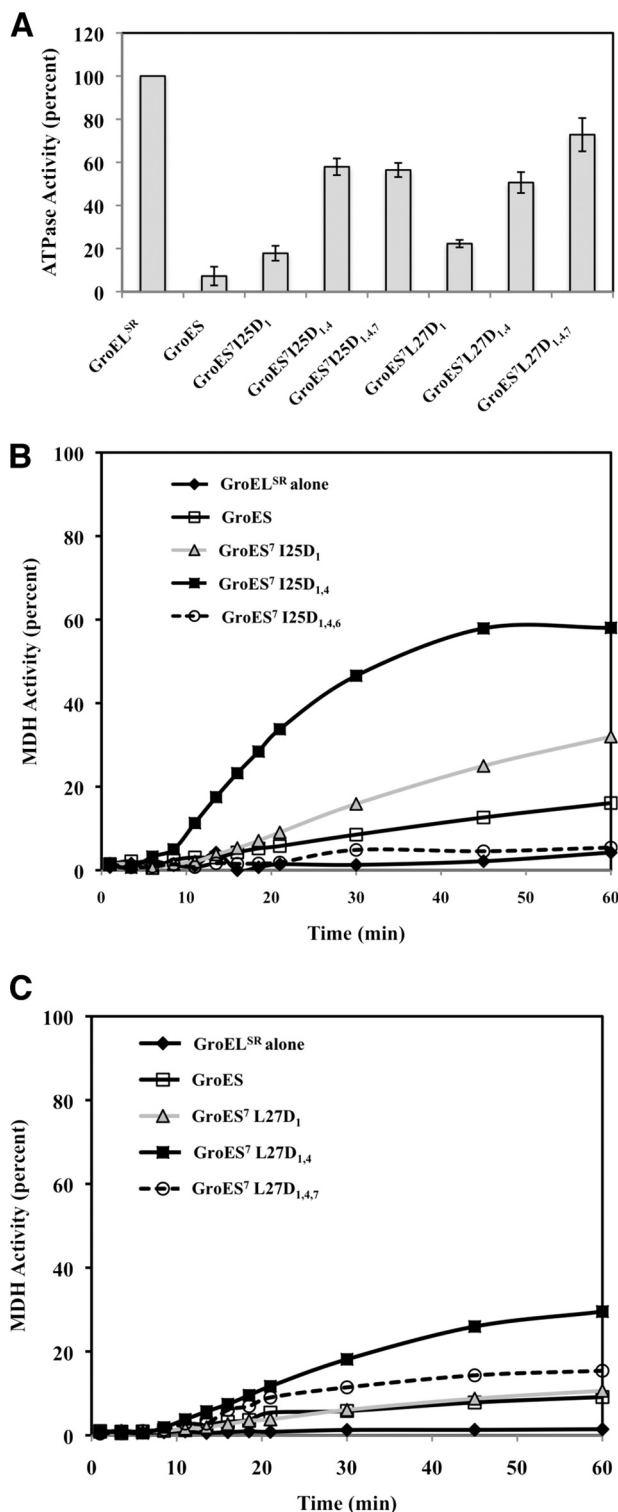


FIGURE 4. Effects of GroES⁷I25D and GroES⁷L27D variants on GroEL^{SR}. *A*, steady-state ATPase activity. *B* and *C*, MDH folding activity. For the ATPase experiments, the intrinsic GroEL^{SR} ATP hydrolysis rate was set as 100%. Experiments were repeated at least three times, and S.D. values (error bars) are shown. For the MDH folding assay, activity of native MDH was set as 100%. Experiments were repeated multiple times, and data of representative runs are shown here.

the cochaperonin-induced inhibitory effect, so that GroEL^{SR}-GroES⁷I25D_{1,4} hydrolyzed ATP at a rate 58% that of GroEL^{SR}. Given that GroEL and GroEL^{SR} hydrolyze ATP at the same rate,

the ATPase activity of GroEL^{SR}-GroES⁷I25D_{1,4} was comparable with that of the canonical GroEL-GroES system. Interestingly, an additional I25D substitution did not further relieve the inhibition, and GroES⁷I25D_{1,4,7} reduced the ATPase activity of GroEL^{SR} to a similar extent, 56%, as GroES⁷I25D_{1,4}. In comparison, the regained ATP hydrolysis activity appeared to increase with the number of L27D substitution, with 22, 51, and 73% GroEL^{SR} activity for systems using GroES⁷L27D₁, GroES⁷L27D_{1,4}, and GroES⁷L27D_{1,4,7}, respectively (Fig. 4A). Also note that GroES⁷L27D_{1,4} regulated GroEL^{SR} ATP hydrolysis at a rate similar to GroES regulation of GroEL. The elevated ATP hydrolysis rates of GroEL^{SR} observed using variants of GroES⁷I25D and GroES⁷L27D suggest efficient turnover of the folding chamber of the single ring GroEL^{SR}, or dissociation of GroEL^{SR} and GroES⁷ at a biologically relevant time frame. As expected, V26D substitutions in GroES⁷ did not effectively revive the ATP hydrolysis rate of the system (supplemental Fig. S2B), suggesting that GroEL^{SR} remained arrested in the highly stable complex state.

Stimulating Substrate Folding Activity of GroEL^{SR}—With the regained ATP hydrolysis using variants of GroES⁷I25D and GroES⁷L27D, the GroEL^{SR} folding chamber presumably has a revived turnover cycle and might support MDH folding. An increase of folding yield to 32% was observed using the single I25D-substituted GroES⁷I25D₁ over a 60-min time course, from ~15% of GroEL^{SR}-GroES (Fig. 4B). Most strikingly, the MDH folding yield continued to improve to >50% during the 60-min assay period when using the double-substituted GroES⁷I25D_{1,4}. This improved MDH yield achieved by the single ring system corresponded to ~70% of the maximum folding yield (~77%) using the canonical double ring GroEL-GroES system. It is noted that the MDH folding accelerated drastically after the first 10-min delay (Fig. 4B). An additional I25D substitution, GroES⁷I25D_{1,4,7}, however, completely abolished the regained MDH folding activity. Intriguingly, of the three GroES⁷L27D variants tested, only GroES⁷L27D_{1,4} improved MDH folding substantially with a final folding yield of ~30% (Fig. 4C). GroES⁷L27D₁, which allowed ATP to hydrolyze at a rate much higher than GroES (or GroES⁷I25D₁), did not increase MDH folding significantly compared with GroES. MDH folding in the presence of GroES⁷V26D variants and GroEL^{SR} was not improved compared with that using GroES-GroEL^{SR} (supplemental Fig. S3B). Our observations that substitutions at Ile-25 in GroES⁷ are more effective than those at Val-26 or Leu-27 in activating MDH folding activity of GroEL^{SR} parallel results from genetic studies (36). In their work, Liu *et al.* substituted each of Ile-25, Val-26, and Leu-27 to 19 other amino acids and assayed the abilities of these GroES variants and GroEL^{SR} to support cell growth. They found that only GroES variants with Ile-25 substitutions may collaborate with GroEL^{SR} to support cell growth.

DISCUSSION

Among the various aspects that the chaperonins may contribute to substrate protein folding efficiency, the distinctive ability to provide a folding favorable isolated environment (the *cis* folding chamber) for protein folding is fundamental (51). Presumably, efficient turnover of the folding chamber is critical

during cell growth; the extremely slow GroEL^{SR}-GroES reaction cycle ($t_{1/2} \sim 300$ min) does not meet the demand by cellular proteins for folding and fails to support cell growth. Turnover of the folding chamber is driven by ATP action, and the rate-limiting step of the GroEL-GroES steady-state ATPase reaction is the departure of GroES (25). Dissociation of GroES in the *cis* folding chamber, however, is also affected by the presence of substrate proteins, as it is stimulated greatly (by 20–50-fold) by binding of substrate proteins to the *trans* GroEL ring (52).

However, efficient turnover of the folding chamber may not be the only factor for effective chaperonin function. In this study, we show that variants of GroES⁷ can rescue the ATPase function of GroEL^{SR}; however, they do not always restore the substrate (MDH) folding activity of GroEL^{SR}. Both GroES⁷I25D₁ and GroES⁷L27D₁ improve ATPase activity of GroEL^{SR} from <10% to ~20% of the intrinsic rate of GroEL^{SR}; however, only GroES⁷I25D₁ improves MDH folding significantly, whereas GroES⁷L27D₁ remains ineffective in MDH folding. Moreover, although three GroES⁷ variants, GroES⁷I25D_{1,4}, GroES⁷I25D_{1,4,7}, and GroES⁷L27D_{1,4}, further increase ATP hydrolysis rate of GroEL^{SR} to a similar level (~50% of the intrinsic rate), which is comparable with the canonical GroEL-GroES system, their abilities in assisting MDH folding vary drastically. With two substitutions in the same GroES modules, GroES⁷I25D_{1,4} is able to support GroEL^{SR}-assisted MDH folding more effectively and efficiently than GroES⁷L27D_{1,4} (Fig. 4, B and C). GroES⁷I25D_{1,4,7}, despite its additional I25D substitution, regulates the ATP hydrolysis rate of single ring GroEL^{SR} to the same extent as GroES⁷I25D_{1,4}. This observation is particularly intriguing because GroES⁷I25D_{1,4,7} is expected to have a weaker effect than GroES⁷I25D_{1,4} on the ATPase rate of GroEL^{SR} as observed when using GroEL (Fig. 3A). More strikingly, although GroES⁷I25D_{1,4} improves MDH folding activity of GroEL^{SR} with a remarkable reaction kinetic and folding yield, GroES⁷I25D_{1,4,7} fails to collaborate with GroEL^{SR} to fold MDH. Given that all of the substitutions (I25D and L27D) are on the cochaperonin and are limited to the GroEL-GroES interface, our findings suggest a direct, specific functional role of GroEL-GroES interaction in promoting substrate folding.

Dynamics of GroES with GroEL have been shown to correlate with molecular events along the folding reaction of the substrate proteins within the folding cavity. Following an initial rapid association step, GroES displays two kinetic phases in interacting with GroEL (32, 53, 54), and these two processes are correlated with the initiation and termination steps of substrate folding inside the protected chamber. Specifically, it is shown that the substrate protein continues ongoing association with GroEL during the initial binding of GroES to form the *cis* GroEL-substrate-GroES ternary complex (55–57). Further action of GroES is required to release the chaperonin-bound substrate completely into the newly formed enclosed folding chamber, which initiates the folding event of the substrate protein (57, 58). The process of this action, observed as the first phase of the GroEL-GroES kinetics with a lifetime of τ_1 , is correlated with releasing substrate into the cavity for folding (32). The liberated substrate protein continues folding within the protected cavity for a time period of 8–15 s (20, 24, 25, 30, 52)

until it is ejected from the chaperonin system due to GroES departure. The time frame that substrate protein is allowed to fold within the enclosed chamber aligns with the second phase of the GroEL-GroES kinetics (with a lifetime of τ_2) (32). In other words, of the entire time frame GroES interacting with GroEL (a lifetime of $\tau_1 + \tau_2$), substrate proteins start folding after a delay of τ_1 and continue folding for an average time of τ_2 . For the chaperonin systems with the same overall reaction kinetics ($\tau_1 + \tau_2$), a simple mechanism for optimal protein folding would be a short τ_1 and with productive release of substrate and an extended τ_2 for folding in the protective environment. In this study, as suggested by the similar rates of the ATPase cycle (Fig. 4A), the overall reaction kinetics of GroEL^{SR} with three GroES⁷ variants, GroES⁷I25D_{1,4}, GroES⁷L27D_{1,4}, and GroES⁷I25D_{1,4,7}, is similar, and is comparable with the functionally optimized GroEL-GroES. Their differences in MDH folding properties (above) may be explained by their abilities to productively displace MDH into the isolated folding chamber for folding. For example, compared with GroES⁷I25D_{1,4}, the further reduced affinity of GroES⁷I25D_{1,4,7} for GroEL^{SR} may not release MDH completely (*i.e.* having a long delay of τ_1) or may not discharge MDH to folding productive conformations, resulting in its inability to activate MDH folding of GroEL^{SR}. Similarly, the different GroEL^{SR}-mediated MDH folding activities between GroES⁷I25D_{1,4} and GroES⁷L27D_{1,4} and those between GroES⁷I25D₁ and GroES⁷L27D₁ can be explained by the distinctive effects of Ile-25 and Leu-27 on the efficiency of displacing substrate into the folding chamber or on the GroEL-GroES interaction dynamics. However, it is not clear why GroES⁷I25D variants cause greater effects on both GroEL- and GroEL^{SR}-assisted MDH folding than the corresponding GroES⁷L27D variants.

Although the slow turnover of the GroEL^{SR}-GroES folding cavity as observed by the diminishing ATPase activity may account for the inability of GroEL^{SR}-GroES to assist protein folding, we demonstrate in this study that a normal ATP function is not sufficient and that an interplay between GroES and GroEL directly impacts the folding reaction of the substrate proteins. Our newly generated *groES*⁷ provides a toolbox to dissect molecular events of protein folding inside the folding chamber and to identify the dynamic aspects of the folding chamber that are critical to improving folding of substrate proteins. Studies using variants of GroES⁷ in conjunction with GroEL^{SR} may provide insightful information to mtHsp60-mtHsp10, the GroEL-GroES counter part in mammalian mitochondria.

REFERENCES

1. Sigler, P. B., Xu, Z., Rye, H. S., Burston, S. G., Fenton, W. A., and Horwich, A. L. (1998) *Annu. Rev. Biochem.* **67**, 581–608
2. Thirumalai, D., and Lorimer, G. H. (2001) *Annu. Rev. Biophys. Biomol. Struct.* **30**, 245–269
3. Saibil, H. R., and Ranson, N. A. (2002) *Trends Biochem. Sci.* **27**, 627–632
4. Hartl, F. U., and Hayer-Hartl, M. (2002) *Science* **295**, 1852–1858
5. Horwich, A. L., Farr, G. W., and Fenton, W. A. (2006) *Chem. Rev.* **106**, 1917–1930
6. Lin, Z., and Rye, H. S. (2006) *Crit. Rev. Biochem. Mol. Biol.* **41**, 211–239
7. Fayet, O., Ziegelhoffer, T., and Georgopoulos, C. (1989) *J. Bacteriol.* **171**, 1379–1385
8. Braig, K., Otwinowski, Z., Hegde, R., Boisvert, D. C., Joachimiak, A., Hor-

- wich, A. L., and Sigler, P. B. (1994) *Nature* **371**, 578–586
9. Fenton, W. A., Kashi, Y., Furtak, K., and Horwich, A. L. (1994) *Nature* **371**, 614–619
 10. Buckle, A. M., Zahn, R., and Fersht, A. R. (1997) *Proc. Natl. Acad. Sci. U.S.A.* **94**, 3571–3575
 11. Chen, L., and Sigler, P. B. (1999) *Cell* **99**, 757–768
 12. Farr, G. W., Furtak, K., Rowland, M. B., Ranson, N. A., Saibil, H. R., Kirchhausen, T., and Horwich, A. L. (2000) *Cell* **100**, 561–573
 13. Hunt, J. F., Weaver, A. J., Landry, S. J., Gierasch, L., and Deisenhofer, J. (1996) *Nature* **379**, 37–45
 14. Mande, S. C., Mehra, V., Bloom, B. R., and Hol, W. G. (1996) *Science* **271**, 203–207
 15. Chandrasekhar, G. N., Tilly, K., Woolford, C., Hendrix, R., and Georgopoulos, C. (1986) *J. Biol. Chem.* **261**, 12414–12419
 16. Todd, M. J., Viitanen, P. V., and Lorimer, G. H. (1993) *Biochemistry* **32**, 8560–8567
 17. Viitanen, P. V., Lubben, T. H., Reed, J., Goloubinoff, P., O'Keefe, D. P., and Lorimer, G. H. (1990) *Biochemistry* **29**, 5665–5671
 18. Gray, T. E., and Fersht, A. R. (1991) *FEBS Lett.* **292**, 254–258
 19. Xu, Z., Horwich, A. L., and Sigler, P. B. (1997) *Nature* **388**, 741–750
 20. Rye, H. S., Burston, S. G., Fenton, W. A., Beechem, J. M., Xu, Z., Sigler, P. B., and Horwich, A. L. (1997) *Nature* **388**, 792–798
 21. Jackson, G. S., Staniforth, R. A., Halsall, D. J., Atkinson, T., Holbrook, J. J., Clarke, A. R., and Burston, S. G. (1993) *Biochemistry* **32**, 2554–2563
 22. Hayer-Hartl, M. K., Martin, J., and Hartl, F. U. (1995) *Science* **269**, 836–841
 23. Nielsen, K. L., and Cowan, N. J. (1998) *Mol. Cell* **2**, 93–99
 24. Todd, M. J., Viitanen, P. V., and Lorimer, G. H. (1994) *Science* **265**, 659–666
 25. Burston, S. G., Ranson, N. A., and Clarke, A. R. (1995) *J. Mol. Biol.* **249**, 138–152
 26. Lorimer, G. (1997) *Nature* **388**, 720–721, 723
 27. Sparrer, H., Rutkat, K., and Buchner, J. (1997) *Proc. Natl. Acad. Sci. U.S.A.* **94**, 1096–1100
 28. Kad, N. M., Ranson, N. A., Cliff, M. J., and Clarke, A. R. (1998) *J. Mol. Biol.* **278**, 267–278
 29. Weissman, J. S., Hohl, C. M., Kovalenko, O., Kashi, Y., Chen, S., Braig, K., Saibil, H. R., Fenton, W. A., and Horwich, A. L. (1995) *Cell* **83**, 577–587
 30. Weissman, J. S., Rye, H. S., Fenton, W. A., Beechem, J. M., and Horwich, A. L. (1996) *Cell* **84**, 481–490
 31. Hayer-Hartl, M. K., Weber, F., and Hartl, F. U. (1996) *EMBO J.* **15**, 6111–6121
 32. Ueno, T., Taguchi, H., Tadakuma, H., Yoshida, M., and Funatsu, T. (2004) *Mol. Cell* **14**, 423–434
 33. Weber, F., Keppel, F., Georgopoulos, C., Hayer-Hartl, M. K., and Hartl, F. U. (1998) *Nat. Struct. Biol.* **5**, 977–985
 34. Chatellier, J., Hill, F., Foster, N. W., Goloubinoff, P., and Fersht, A. R. (2000) *J. Mol. Biol.* **304**, 897–910
 35. Sun, Z., Scott, D. J., and Lund, P. A. (2003) *J. Mol. Biol.* **332**, 715–728
 36. Liu, H., Kovács, E., and Lund, P. A. (2009) *FEBS Lett.* **583**, 2365–2371
 37. Kovács, E., Sun, Z., Liu, H., Scott, D. J., Karsisiotis, A. I., Clarke, A. R., Burston, S. G., and Lund, P. A. (2010) *J. Mol. Biol.* **396**, 1271–1283
 38. Viitanen, P. V., Lorimer, G. H., Seetharam, R., Gupta, R. S., Oppenheim, J., Thomas, J. O., and Cowan, N. J. (1992) *J. Biol. Chem.* **267**, 695–698
 39. Nielsen, K. L., McLennan, N., Masters, M., and Cowan, N. J. (1999) *J. Bacteriol.* **181**, 5871–5875
 40. Viitanen, P. V., Lorimer, G., Bergmeier, W., Weiss, C., Kessel, M., and Goloubinoff, P. (1998) *Methods Enzymol.* **290**, 203–217
 41. Todd, M. J., Walke, S., Lorimer, G., Truscott, K., and Scopes, R. K. (1995) *Biochemistry* **34**, 14932–14941
 42. Li, Y., Zheng, Z., Ramsey, A., and Chen, L. (2010) *J. Pept. Sci.* **16**, 693–700
 43. Lanzetta, P. A., Alvarez, L. J., Reinach, P. S., and Candia, O. A. (1979) *Anal. Biochem.* **100**, 95–97
 44. Ranson, N. A., Burston, S. G., and Clarke, A. R. (1997) *J. Mol. Biol.* **266**, 656–664
 45. Motojima, F., Makio, T., Aoki, K., Makino, Y., Kuwajima, K., and Yoshida, M. (2000) *Biochem. Biophys. Res. Commun.* **267**, 842–849
 46. Suzuki, M., Ueno, T., Iizuka, R., Miura, T., Zako, T., Akahori, R., Miyake, T., Shimamoto, N., Aoki, M., Tanii, T., Ohdomari, I., and Funatsu, T. (2008) *J. Biol. Chem.* **283**, 23931–23939
 47. Ben-Zvi, A. P., Chatellier, J., Fersht, A. R., and Goloubinoff, P. (1998) *Proc. Natl. Acad. Sci. U.S.A.* **95**, 15275–15280
 48. Gupta, R. S. (1996) in *The Chaperonins* (Ellis, R. J., ed) pp. 27–64, Academic Press, San Diego
 49. Sakane, I., Hongo, K., Motojima, F., Murayama, S., Mizobata, T., and Kawata, Y. (2007) *J. Mol. Biol.* **367**, 1171–1185
 50. Nojima, T., Murayama, S., Yoshida, M., and Motojima, F. (2008) *J. Biol. Chem.* **283**, 18385–18392
 51. Brinker, A., Pfeifer, G., Kerner, M. J., Naylor, D. J., Hartl, F. U., and Hayer-Hartl, M. (2001) *Cell* **107**, 223–233
 52. Rye, H. S., Roseman, A. M., Chen, S., Furtak, K., Fenton, W. A., Saibil, H. R., and Horwich, A. L. (1999) *Cell* **97**, 325–338
 53. Viani, M. B., Pietrasanta, L. I., Thompson, J. B., Chand, A., Gebeshuber, I. C., Kindt, J. H., Richter, M., Hansma, H. G., and Hansma, P. K. (2000) *Nat. Struct. Biol.* **7**, 644–647
 54. Taguchi, H., Ueno, T., Tadakuma, H., Yoshida, M., and Funatsu, T. (2001) *Nat. Biotechnol.* **19**, 861–865
 55. Cliff, M. J., Kad, N. M., Hay, N., Lund, P. A., Webb, M. R., Burston, S. G., and Clarke, A. R. (1999) *J. Mol. Biol.* **293**, 667–684
 56. Kawata, Y., Kawagoe, M., Hongo, K., Miyazaki, T., Higurashi, T., Mizobata, T., and Nagai, J. (1999) *Biochemistry* **38**, 15731–15740
 57. Cliff, M. J., Limpkin, C., Cameron, A., Burston, S. G., and Clarke, A. R. (2006) *J. Biol. Chem.* **281**, 21266–21275
 58. Miyazaki, T., Yoshimi, T., Furutsu, Y., Hongo, K., Mizobata, T., Kanemori, M., and Kawata, Y. (2002) *J. Biol. Chem.* **277**, 50621–50628